SARCOMERE LENGTH DETERMINATION USING LASER DIFFRACTION

Effect of Beam and Fiber Diameter

RICHARD L. LIEBER, YIN YEH, AND RONALD J. BASKIN
Departments of Zoology and Applied Science, University of California, Davis, California 95616

ABSTRACT An experimental and theoretical analysis is presented involving the effect of variation in fiber and beam diameter upon the determination of average sarcomere length in isolated single muscle fibers using laser light diffraction. The muscle diffraction phenomenon is simplified by first considering diffraction order position and intensity to be the result of grating and Bragg diffraction. It is the product of the intensity profiles, which results from these types of diffraction, that produces the diffracted order. These simplifying assumptions are then extended to the case of the real muscle. Based on these considerations and the theory that we recently presented, conditions are set forth under which grating information (i.e., sarcomere length) can be maximally expressed to yield accurate average sarcomere length values.

INTRODUCTION

The use of laser diffraction is ubiquitous in present day muscle physiology investigations (Cleworth and Edman, 1972; Kawai and Kunz, 1973; Schoenberg et al., 1974; Borejdo and Mason, 1976; Paolini et al., 1976; Moss and Halpern, 1977; Flitney and Hirst, 1978; Rüdel and Zite-Ferenczy, 1979; Walcott and Dewey, 1980, Magid and Reedy, 1980; Edman, 1980; Baskin et al., 1981). The location of strong diffraction intensity maxima can be analyzed in a straightforward manner to provide a measurement of the average sarcomere length. These sarcomere length measurements are generally considered adequate until experimental results require a high degree of accuracy. Observed line splitting, changes in intensity, and even changes in spatial location of the diffraction peaks are subject to varied interpretation.

Rüdel and Zite-Ferenczy (1979*a*) have postulated that Bragg plane reflections are responsible for the observed intensity asymmetry in single skeletal muscle fibers. Their work was based on observations of the intensity variations of the left and right first-order diffraction patterns as a function of incident angle (ω-scan). For certain well-defined incident angles, strong intensity peaks were observed. The explanation advanced was that a Bragg reflecting plane condition had been met for the fiber of sarcomere length L and angle ω.

A theory of light diffraction by muscle fibers was put forth by Yeh et al. (1980). It was proposed that the diffraction pattern observed is indeed a combination of interference conditions met by (*a*) rows of myofibrils composed of sarcomeres spaced at sarcomere length L, and (*b*) parallel myofibrils whose sarcomeres are out of register with respect to their neighbors by a fixed amount. This theory has been tested experimentally and shown to describe (*a*) diffracted intensity and position as a function of sarcomere length (Baskin et al., 1979), (*b*) diffracted intensity as a function of incident angle (Baskin et al., 1981), and (*c*) diffracted intensity changes upon stimulation of intact (Baskin et al., 1979) and mechanically or chemically activated fibers (Oba et al., 1981). In the present work, the theory of Yeh et al. (1980) is used to predict the optimal conditions (beam and fiber diameter) for measurement of sarcomere length using laser diffraction. Portions of this work have been previously reported (Lieber et al., 1981).

THEORETICAL BACKGROUND

Based on a model of a single sarcomere population (i.e., one sarcomere length and one skew angle, Yeh et al., 1980; Baskin et al., 1981) the intensity of diffracted light in the meridional direction (Fig. 1) may be given as

$$I_\ell(R) = I_s |G_\ell(q_z)|^2 |H(A)|^2, \quad (1)$$

where R is the distance from the scattering site (the fiber) to the detector, and ℓ is the order of the diffraction pattern. Of the three factors, the first one, I_s, represents the contribution from a single scattering center weighted by the form factor. The form factor arises from the cylindrical geometry of the fiber and is evaluated in the plane of scattering, which

Address for correspondence to Dr. Lieber, Department of Surgery, Division of Orthopaedics, Veteran's Administration Medical Center, 3350 La Jolla Village Drive, San Diego, California 92161.

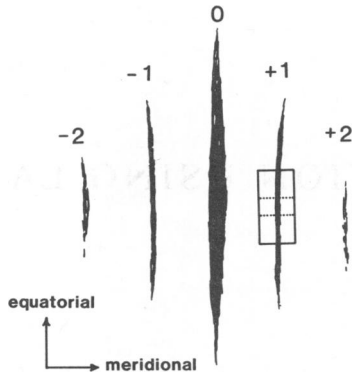

FIGURE 1 Schematic representation of experiments performed. Pictured is a diffraction pattern with the photodetectors placed as during an experiment (not to scale). *ω-scan:* photodiode (solid-lined rectangle on +1 order) is in a fixed position to measure intensity of the diffracted order. Incident angle is varied and intensity vs. incident angle is plotted on an X-Y plotter (Fig. 4). *Diffraction angle vs. incident angle at constant sarcomere length:* photodiode (solid-lined rectangle on +1 order) is in a fixed position to measure position in the meridional direction. Incident angle is varied and meridional angle vs. incident angle is plotted on an X-Y plotter (Fig. 5). *Intensity variabilty across an order as a function of incident angle:* a charge-coupled device (CCD, dotted rectangle on +1 order) measures the intensity profile of the order in the meridional direction. Incident angle is varied and the change in intensity profile vs. incident angle is stored in the microcomputer memory at ~0.8° intervals. These data are then displayed on an oscilloscope and photographed sequentially (Figs. 7–9).

includes the fiber axis. Although the fiber is slightly elliptical in cross section, this does not introduce serious experimental problems. For example, Leung et al. (1983) have successfully correlated intensity oscillations along a diffracted order with average myofibrillar diameter assuming cylindrical cross section. Deviation from cylindrical cross section would only result in changes in the diffraction pattern in the equatorial direction and would not, therefore, affect sarcomere length measurement.

The second factor, $|G_\ell(\mathbf{q}_z)|^2$, represents the intensity profile in the meridional direction (z-direction) due only to the sarcomere periodicity. Here

$$|G_\ell(\mathbf{q}_z)|^2 \equiv \left\{ \frac{\left[p \sin\left(\mathbf{q}_z - \ell K\right) \frac{p}{2} \right]}{\left(\mathbf{q}_z - \ell K\right) \frac{p}{2}} \right\}^2, \qquad (2)$$

where p is the beam diameter along the length of the fiber, $\mathbf{q}_z$ is the scattering vector in the plane of scattering, and $K = (2\pi)/(\text{sarcomere length})$ is a measure of the sarcomere repeat distance in the fiber. One notes that the peak of the ℓth-order diffraction intensity is reached when $\mathbf{q}_z = \ell K$. If $p \rightarrow \infty$, then as the diffraction condition is met, the intensity increases in a δ-function fashion. If p is finite, $|G_\ell(\mathbf{q}_z)|^2$ will exhibit damped oscillatory behavior in angle space or $\mathbf{q}_z$ (Fig. 2 *C* and *D*).

The last factor of Eq. 1, $|H(A)|^2$, represents contribution to the diffraction intensity by the misalignment (skew) of neighboring planes of myofibrils. The type of skew dealt with in the present model is that of a single skew angle throughout the entire fiber. (The case of multiple skew planes within the fiber would represent a more realistic geometrical representation of the fiber. However, this solution cannot be solved in a closed form and will be considered in a later report.) The effect of multiple skew planes would be to smear out the theoretical ω-scan. For the case of the single skew plane

$$|H(A)|^2 = \left[\frac{\sin \frac{NA}{2}}{\sin \frac{A}{2}} \right]^2, \qquad (3)$$

where N is the number of myofibrils forming this skew plane and A measures the extent of the skew projected in the specific $\mathbf{q}_z$-direction. Once again, as in Eq. 2, strong peaking of this factor occurs when N is large. For small values of N, $|H(A)|^2$ exhibits damped oscillatory behavior, here governed by the magnitude of $A/2$ (Fig. 2 *B* and *D*).

In the experiments presented here, beam diameter is varied to change the value of p. Fibers of different thicknesses are used to provide a variation in N. In Fig. 2, four different combinations of N and p are used to schematically represent the expected intensity profile according to Eq. 1. This figure illustrates the intensity profile in reciprocal space near a diffracted order.

In general, the intensity profile due to Bragg diffraction from skew planes may or may not occur at the same meridional location as the intensity profile due to sarcomere periodicity. If the two profiles are at the same meridional angle (solid profiles in Fig. 2), the resulting

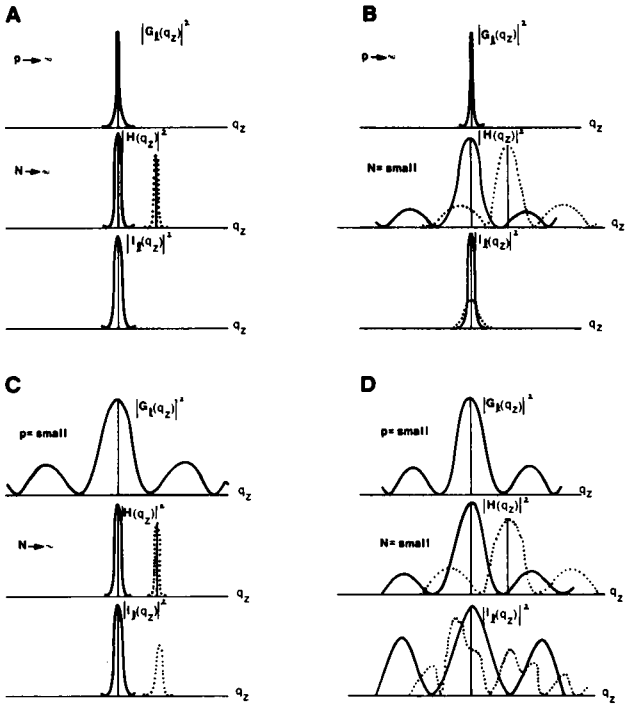

FIGURE 2 Schematic diagram in reciprocal space of the theoretical product of grating and Bragg intensity profiles under different conditions. The amplitudes of the curves are not to scale. $|G_\ell(\mathbf{q}_z)|^2$ represents the grating intensity profile, $|H(A)|^2$ represents the Bragg intensity profile, and $I_\ell(\mathbf{q}_z)$ represents their product. Solid line for $|H(A)|^2$ represents the case where the grating and Bragg intensity profiles exactly overlap, resulting in solid line for $I_\ell(\mathbf{q}_z)$. Dotted line for $|H(A)|^2$ represents the case where grating and Bragg profiles do not exactly overlap, resulting in dotted line for $I_\ell(\mathbf{q}_z)$. (*A*) Beam width (p) and the number of myofibrils (N) approach infinity. (*B*) Beam width approaches infinity, the number of myofibrils is small. (*C*) Beam width is small, number of myofibrils approaches infinity. (*D*) Beam width and number of myofibrils is small.

diffraction pattern provides an accurate measure of the average sarcomere length in the illuminated volume. If the two profiles are not at the same meridional angle (dotted profiles in Fig. 2), the resultant diffraction pattern will provide an accurate measure of average sarcomere length only if the profile due to sarcomere periodicity (grating profile) dominates the profile due to skew planes (Bragg profile, Fig. 2*B*). For all other cases (Figs. 2 *A, C, D*), the accuracy of the technique cannot be guaranteed.

Thus, the product of two simultaneous interference conditions (grating and Bragg-type interference) yields the final intensity profile measured by a photodetector. In making sarcomere length measurements, it is desirable to set experimental conditions such that the grating intensity profile dominates the Bragg profile. Because the spatial location of the Bragg intensity profile is unpredicatable from fiber to fiber (Baskin et al., 1981), expression of average sarcomere length can be insured only by increasing the beam width and using fibers of small diameter to be sure that the number of sarcomeres illuminated is large relative to the number of myofibrils. From a theoretical standpoint, the ideal condition is thus a single myofibril illuminated by a infinitely wide laser. Conversely, with large fibers, the Bragg intensity profile will be large and can dominate the grating profile resulting in an interference pattern that is not representative of the average sarcomere length within the illuminated region. Thus, our experimental approach is to vary beam width and fiber diameter under different experimental conditions to investigate the interaction between grating and Bragg diffraction.

METHODS

The single fibers used in this experiment were dissected from the semitendinosus muscle of the frog (*Rana pipiens*) in Ringer's solution composed of (in millimoles per liter): NaCl (115), KCl (2.5), Na_2HPO_4 (2.15), Na_2HPO_4 (0.85), $CaCl_2$ (1.8), adjusted to pH 7.0. After dissection, the major diameter of the fiber was measured with a Bausch and Lomb calibrated graticule (Bausch and Lomb Inc., Instruments and Systems Div., Rochester, NY) in combination with a Zeiss precision calibrated ruling (Carl Zeiss Inc., Thornwood, NY). The fibers are elliptically shaped. Thus, if any twisting occurs, the diameter of the fiber illuminated might be underestimated. Problems of this type were avoided by carefully aligning the fiber under a dissecting microscope so the major diameter was perpendicular to foil clips applied to the tendons. In this way, the major diameter of the fiber could be reliably positioned with respect to the incident laser beam. All fiber diameters reported are the major fiber diameter. In the cases where the diameter varied along the fiber, Bio-Beads (Bio-Rad Laboratories, Richmond, CA) were used to mark the region of interest. The fiber was observed at low magnification under a phase microscope and selected for clear striations, although not for striation uniformity. The fiber was then placed in the diffraction chamber (Fig. 3*A*) as previously described (Baskin et al., 1981). After the experiment (2–5 h), the fiber was replaced under the microscope and rechecked for clear striations. Only the data from those fibers that showed clear striations throughout the experiment were used (~50% of all fibers used). Loss of striations was usually accompanied by a decrease in the intensity and sharpness of the diffraction pattern. This damage probably occurred during dissection or mounting.

Beam width was varied using a 100-μm diam precision pinhole (Oriel Corp. of America, Stamford, CT) placed ~10 mm under the fiber. Diffraction by the pinhole expanded the zeroth order to ~120 μm at the fiber. Higher order diffraction rings were of negligible intensity. Three different types of diffraction experiments were performed in this study. In each case, the position or intensity across a diffraction order was measured as a function of incident angle. The details for each type of experiment will be discussed sequentially.

ω-Scan

The ω-scan measures the intensity of a diffracted order as a function of incident angle (Fig. 3 *A*) (Rüdel and Zite-Ferenczy, 1979*a*). The system

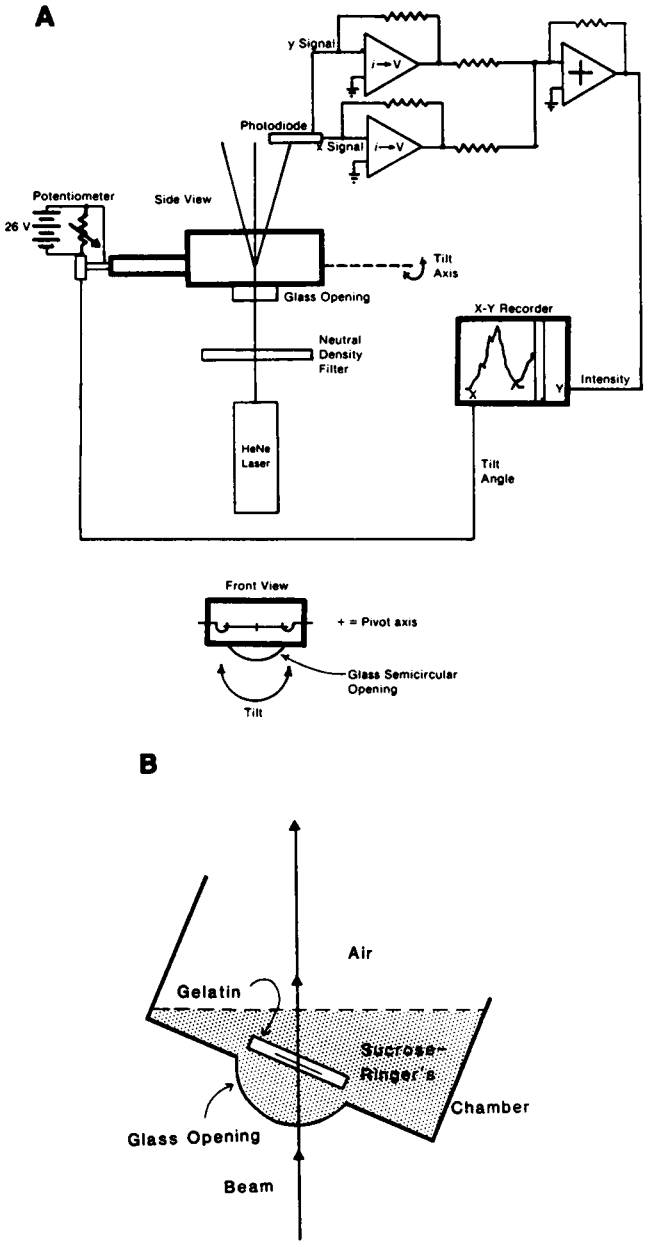

FIGURE 3 (*A*) Schematic diagram of experimental apparatus to monitor diffraction patterns as a function of incident angle. Single fiber is positioned at the intersection of the axis of rotation and the laser beam. Apparatus shown configured to measure and plot intensity. (*B*) Refractive index matching of gelatin slab in Ringer's solution (see text for details). Refractive index of gelatin slab and sucrose-Ringer's solution are both 1.3494 eliminating refraction at their interface.

used was essentially the same as that of Baskin et al. (1981). Because we were attempting to look at small intensity fluctuations and decided to use small incident beams (which were difficult to keep centered on the fiber throughout the scan), it was necessary to modify the apparatus slightly. Modifications allowed us to more precisely and accurately measure incident angle and center a fiber in a small beam throughout the incident angle range. The potentiometer, which was originally used to detect incident angle, was replaced with a precision gearing arrangement. In this configuration, the shaft of the chamber was fitted with a 90-tooth

gear and the shaft of a 10-turn precision potentiometer was fitted with a 20-tooth gear yielding a gear ratio of 4.5:1. Thus, small changes in chamber angle (i.e., small rotations of the chamber shaft) were amplified and detected using a variable voltage divider. The sensitivity of this arrangement was 20 mV/deg with a linearity of 0.9999. The shaft of the chamber was connected to the shaft of a precision motor (peristaltic pump) resulting in tilting of the chamber, which was automated and repeatable. Movement of the laser beam along a fiber during the ω-scan was <39 μm (three pixel elements) as measured by a photodiode array placed at the level of the fiber on the axis of rotation. The rate of tilt for all of these studies was 0.3 deg/s. The photodiode was calibrated in microwatts using an intensity detector (model 66XLA; Photodyne, Inc., Westlake Village, CA). The output of the photodiode in the summing configuration (to measure intensity) was linear from 1.0 to 200 μW (r = 0.9981) with a sensitivity of 70 mV/μW.

To perform ω-scans using the smaller diameter incident beam, it was necessary to develop a method to center the fiber in the beam and hold it stationary during the scan. It was also critical that the same region of the fiber be illminated when changing beam sizes. Small movements of only 50–100 μm resulted in irreproducibility from scan to scan. To firmly fix the fiber in the chamber, we embedded the fiber in a gelatin-Ringer's solution composed of 1.6 g of reagent grade gelatin per 20 ml of Ringer's solution. The refractive index of the resulting gelatin-Ringer's solution was 1.3494. The refractive index of plain Ringer's solution was 1.3340. Thus, to eliminate refraction at the gelatin-Ringer's solution/Ringer's solution interface, 11.66 g of sucrose was added to 100 ml of the bathing Ringer's solution to increase its refractive index to 1.3494. With this index of refraction matching (Fig. 3 *B*), no attenuation or movement of the beam occurred through a gelatin-Ringer's solution slab in a sucrose-Ringer's solution over the incident angle range −25 to +25° (Fig. 4).

Diffraction Angle vs. Incident Angle at Constant Sarcomere Length

The variation in intensity with angle observed during ω-scans prompted us to determine if the observed variations in intensity were accompanied by variations in angle of a diffracted order (since the angle of the order is

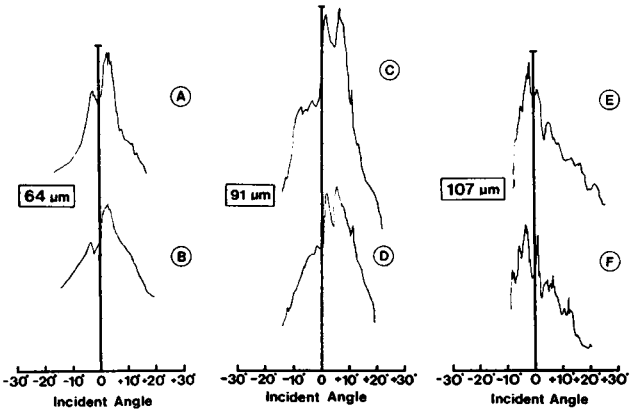

FIGURE 4 ω-scans on three single fibers using beams of two different diameters. Fiber diameter is shown in the box next to the scan. 1-mm beam used on *A*, *C*, and *E*. 100-μm beam used on *B*, *D*, and *E*. (*A*) Fiber diameter equals 64 μm, beam diameter equals 1 mm. Experiment of 6 June 1980. (*B*) Fiber diameter equals 64 μm, beam diameter equals 100 μm. Experiment of 6 June 1980. (*C*) Fiber diameter equals 91 μm, beam diameter equals 1 mm. Experiment of 21 June 1980. (*D*) Fiber diameter equals 91 μm, beam diameter equals 100 μm. Experiment of 21 June 1980. (*E*) Fiber diameter equals 107 μm, beam diameter equals 1 mm. Experiment of 3 July 1980. (*F*) Fiber diameter equals 107 μm, beam diameter equals 100 μm. Experiment of 3 July 1980.

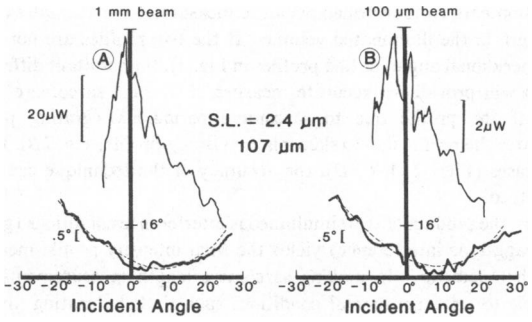

FIGURE 5 Diffraction angle vs. incident angle at constant sarcomere length. *Upper* trace shows ω-scan for region, *lower* trace shows diffraction angle measured. Dashed line in lower trace shows movement of diffracted order predicted by grating equation for arbitrary incident angle. Fiber diameter equals 107 μm, sarcomere length equals 2.4 μm. Experiment of 3 July 1980. (*A*) Beam diameter equals 1 mm. (*B*) Beam diameter equals 100 μm. Note intensity scale differences in *A* and *B*.

used to determine sarcomere length). To measure position with the existing system, the outputs from two of the leads of the photodiode were fed into a difference amplifier. This difference was then divided by the total incident intensity to yield position, independent of intensity (Zite-Ferenczy and Rüdel, 1978). In the position detection mode, it was possible to resolve lateral movement of 100 μm. With the detector positioned 85 mm from a fiber of sarcomere length 2.4 μm, at normal incidence, this corresponded to an angular difference of ~0.07° (corresponding to a length change of 0.011 μm). As the fiber was tilted, the output of the photodiode system was position vs. incident angle. The position of the photodiode on the diffraction order is shown schematically in Fig. 1. As the fiber was tilted, the position of the order in the meridional direction was measured. This position value was converted to an angle and plotted as the ordinate in the lower trace of Fig. 5. These angle data were then converted to apparent sarcomere lengths using the grating equation for arbitrary incident angle

$$n\lambda = d \sin \theta_i + d \sin \theta_d, \quad (4)$$

where n is the diffracted order, λ is the incident wavelength, d is the

FIGURE 6 Sarcomere length vs. incident angle for a single fiber, 73 μm diam. Thin horizontal dashed line represents sarcomere length measured at normal incidence with wide beam (2.503 μm). Dashed data trace obtained using 1-mm incident beam width. Solid data trace obtained using 100-μm incident beam width. Sarcomere length calculated from diffraction angle data taken using planar diffused photodiode. Diffraction angle converted to sarcomere length using Eq. 4.

grating spacing (sarcomere length), θ_i is the incident angle, and θ_d is the diffraction angle. Apparent sarcomere length vs. incident angle was plotted as shown in Fig. 6. Here a 73-μm diam fiber was scanned with the two different beam widths.

Intensity Variability Across an Order Line as a Function of Incident Angle

After several experiments it became clear that we were limited in one aspect by using the photodiode described above. The planar diffused photodiode could only detect the centroid of intensity (or position) of a diffracted order. Thus, one could only detect changes that affect the centroid of intensity or position. It was possible that changes across a diffracted order (in the meridional direction) could occur, but the centroid of the profile remain the same. It was, therefore, desirable to directly monitor the profile of a diffracted order. We accomplished this using the computer system described by Roos et al. (1980) and Lieber and Baskin (1980). This system is a microprocessor that can rapidly acquire diffraction patterns from a linear photodiode array, which performs serial output via a charge-coupled device (CCD). The advantage of this photodetection system is that the intensity profile across a diffracted order

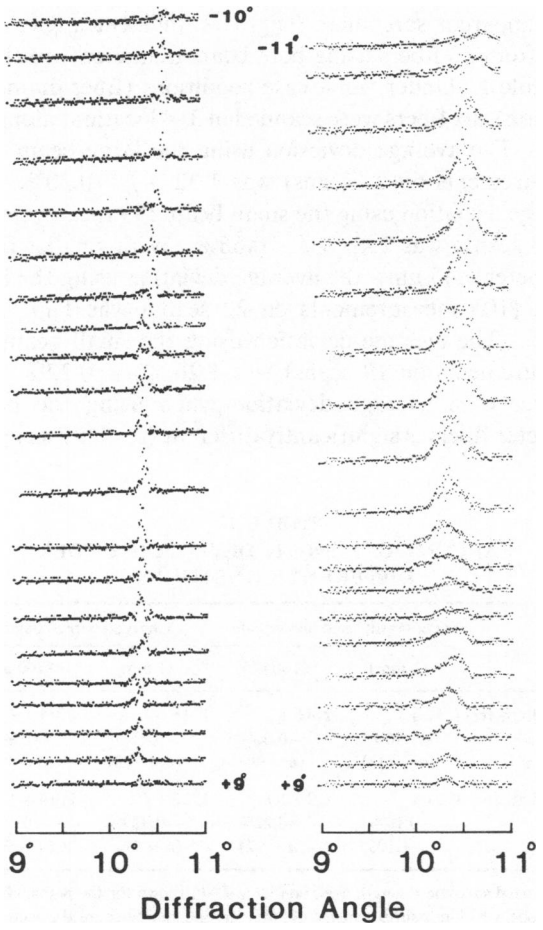

FIGURE 7 Intensity variation across an order as a function of incident angle. 36-μm diam fiber. Sarcomere length equals 3.5 μm. Experiment of 1 July 1981. Gel embedding was not used on this fiber. Each trace taken after ~0.8° of tilt. Diffracted angles shown are only approximate. *Left*: 1-mm incident beam. Fiber tilted over range −10 to +9°. *Right*: 100 μm incident beam. Fiber tilted over range −11 to +9°.

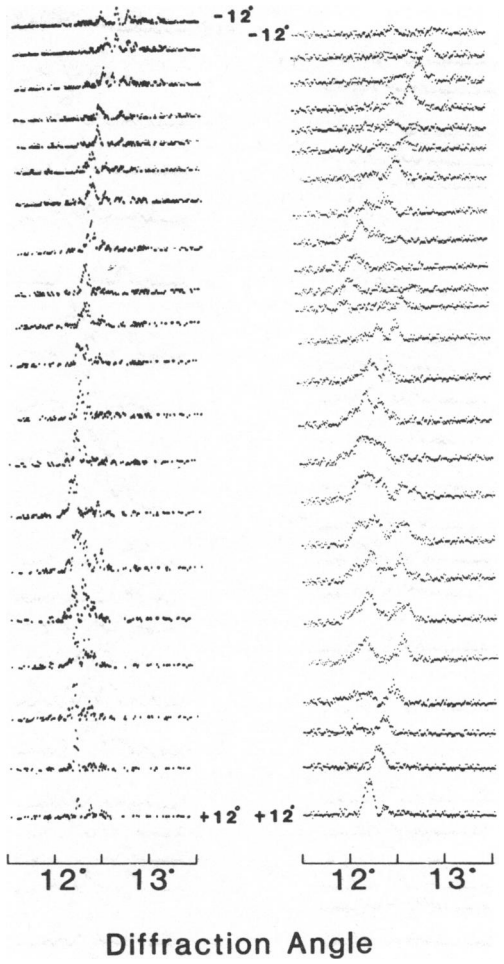

FIGURE 8 Intensity variation across an order as a function of incident angle. 50-μm fiber. Sarcomere length equals 3.0 μm. Experiment of 30 June 1981. Conditions as in Fig. 7. *Left*: 1-mm incident beam. Fiber tilted over range −12 to +12°. *Right*: 100-μm incident beam. Fiber tilted over range −12 to +12°. Note the two major shifts in position of the peak between the 11th and 13th scans and between the 18th and 20th scans in the right but not in the left.

can be measured. The disadvantage of such a detection system is that the aperture of the array is only 17 μm and thus a small sample of the order is taken. In performing this experiment, the fiber was placed in the chamber as described above but the CCD array was substituted as the photodetector (Fig. 1). The chamber tilting motor was started and frames of data were taken at ~0.8° intervals. This provided a series of intensity profiles across a diffracted order as a function of incident angle (Figs. 7–9). In this case, however, the incident angle values were only approximate.

RESULTS

ω-Scans

Fig. 4 shows typical results from ω-scans performed on fibers of different diameters with beams of two different diameters. The top row represents the ω-scans taken with the large beam, and the lower row the ω-scans taken with

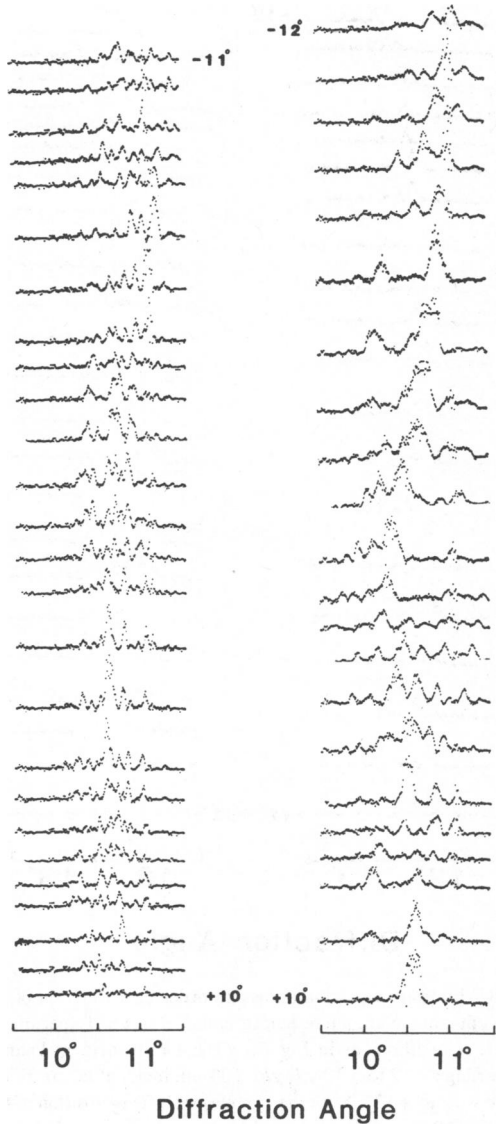

FIGURE 9 Intensity variation across an order as a function of incident angle. 91-μm fiber. Sarcomere length equals 3.5 μm. Experiment of 15 July 1981. Conditions as in Fig. 7. *Left*: 1-mm incident beam. Fiber tilted over range −11 to +10°. *Right*: 100-μm incident beam. Fiber tilted over range −12 to +10°.

the small beam. Note that when the small beam is used with relatively large fibers (Fig. 4 *F*), more fine structure is observed relative to that obtained with the larger beam (Fig. 4 *E*). This difference becomes less pronounced as the fiber diameter is decreased (Fig. 4 *C, D* and *A, B*).

The fine structure peaks observed with the smaller beam do not always correspond to small peaks on the scan with the larger beam. Also, in several experiments, which lasted over 4 h, the profile of the angle scan, as well as the symmetry angle (Baskin et al., 1981) changed, suggesting a major change in internal myofibrillar structure. These changes occurred even in fibers that showed clear striations throughout the experiment.

Diffraction Angle vs. Incident Angle at Constant Sarcomere Length

Because the position of a diffracted order is used to compute a sarcomere length value, it is of interest to determine if the intensity changes observed with ω-scans are correlated with change in position of a diffracted order. To determine the variation in position of a diffracted order, diffraction angle is measured while varying incident angle. Experimental conditions varied are fiber diameter and beam diameter. The results are shown for one fiber in Fig. 5. The upper traces of the figure are the ω-scans for the region of the fiber scanned in the lower traces (same fiber as Fig. 4). Note that the vertical axis for the ω-scan is intensity, while that for the lower trace is diffraction angle. The dashed line in the lower trace represents the movement of a diffracted order as a function of incident angle predicted by the grating equation at arbitrary incident angle (Eq. 4). The solid line represents the angle of the diffracted order as determined by the photodiode system in the position mode. These type of data are replotted in Fig. 6 as apparent sarcomere length vs. incident angle. The data from 23 fibers using both beam diameters are shown in Table I. Under worst case conditions (fiber diameters >90 μm), six fibers were scanned in 3–4 locations along the fiber. The average deviation using the large beam (113 measurements on 23 scans) was 1.32 +/− 0.30%. The average deviation using the small beam (99 measurements on 19 scans) was 2.46 +/− 0.66%. With smaller fibers (diameter <45 μm), the average deviation using the large beam (105 measurements on 22 scans) was 1.11 +/− 0.19%. The average deviation using the small beam (92 measurements on 19 scans) was 1.26 +/− 0.22%. The difference in average deviation when using the larger diameter fibers is significantly different ($p < 0.05$ using the

TABLE I
SARCOMERE LENGTH DEVIATION UNDER DIFFERENT CONDITIONS

	Planar diffused photodiode		Charge-coupled device	
	(1 mm)	(100 μm)	(1 mm)	(100 μm)
Fiber diameter >90 μm	1.32 +/− 0.30%* (n = 113)	2.46 +/− 0.66% (n = 99)	1.45 +/− 0.41%* (n = 110)	2.94 +/− 0.94% (n = 118)
Fiber diameter <45 μm	1.11 +/− 0.19% (n = 105)	1.26 +/− 0.22% (n = 92)	1.22 +/− 0.33% (n = 89)	1.44 +/− 0.36% (n = 93)

Summarized sarcomere length deviation data. Data shown for the planar diffused photodiode, which measures centroid of intensity, and charge-coupled device, which measures intensity distribution. For each type of photodetector, average percent deviation (relative to sarcomere length measured at normal incidence) was calculated for the 100 μm and 1-mm beams (cf. Fig. 6). The data were then subdivided by fiber diameter. Note the significant difference in the average deviation when using different beam diameters and large (>90 μm) fibers. No significant difference is seen when using the small fibers (<45 μm).

*$p < 0.05$, significant difference between deviation with large and small beam widths.

Student's t test). There is not a significant difference in the deviation values obtained using the smaller fibers. Scans were obtained where little difference in the deviation from theory was observed for the two different beam widths, but the reverse situation (more deviation from theoretical with larger beam) was never observed.

Intensity Variability Across an Order Line as a Function of Incident Angle

Because the planar diffused photodiode used above only measures centroid of position, it is possible that some changes in the position of the order might not be detected. Thus to measure the profile as well as the position of a diffracted order, a different type of photodetector is used, the CCD, associated with the system described in Methods. Typical results obtained by varying fiber diameter and beam width are shown in Figs. 7–9. Shown are the intensity across an order at ~0.8° incident angle increments. The two major results of the fibers studied ($n = 48$) are the following.

(*a*) When very large fibers are used (i.e., >90 μm) significant splitting of the diffracted order is always observed. As incident angle is varied, much rapid movement of these various peaks across the CCD detector is observed. This characteristic is dramatic for both the large and small beams (Fig. 9).

(*b*) When very small fibers are used (i.e., <45 μm), almost no peak splitting is observed. As incident angle is varied, the order moves smoothly across the face of the CCD (Fig. 7). For the small beam and small fibers, the diffracted order is not very intense and thus it is difficult to measure a sharp pattern. However, for the larger beam, the diffracted order is narrow and significantly intense to carry out the scan.

Similar analysis was performed on the scans obtained with the CCD device as on the scans obtained with the planar diffused photodiode (Table I). The sarcomere length corresponding to each peak along the CCD profile was calculated for large (>90-μm diam) fibers. For the large beam, the average deviation was determined to be 1.45 +/− 0.41. For the smaller beam, the average deviation was 2.94 +/− 0.94%. When using smaller fibers (fiber diameter <45 μm) the average deviation was 1.22 +/− 0.33% for the large beam and 1.44 +/− 0.36% for the small beam. Again, the results obtained for the large fibers are significantly different (p <0.05), while the results obtained with the smaller fibers are not significantly different. These results are somewhat greater than those obtained with the planar diffused photodiode and indicate that peaks across the diffracted order, which do not appreciably affect the centroid, may occur. While we observe the patterns described above, we emphasize that variation is observed from fiber to fiber. This is apparently a result of the variable nature of the myofibrillar structure within the fiber.

Experimental Summary

A total of 65 experiments on 45 fibers were performed. The summarized data for the scans that measure apparent sarcomere length vs. incident angle at constant sarcomere length are shown in Fig. 10. For these experiments, when the sarcomere length value measured at a certain incident angle deviated from the theoretical value (Eq. 4) by more than 3%, this deviation was considered to be due to three-dimensional effects such as Bragg reflection. A deviation from theory of <3% was considered acceptable because the resting sarcomere length dispersion in the central 90% of the fiber has been shown by phase microscopy and laser diffraction to be 1–2% (A. F. Huxley and Peachey, 1961; Edman, 1966; Kawai and Kunz, 1973; Paolini et al., 1976). For each range of fiber diameter and for both beam diameters, the number of fibers exceeding the 3% limit was determined and the result plotted in a bar graph. The vertical axes of Fig. 10 represents the percent of fibers in a given diameter range that deviate from theory by more than 3%. For example, note that for the fiber data plotted in Fig. 6, the 100-μm beam data shows deviations from theory by more than 3% at several locations, while the 1-mm beam data never exceeds the 3% limit.

For the 100-μm beam, a significant proportion of the fibers deviate from ideal above a diameter of 45 μm. On the other hand, for the 1-mm beam, significant deviation does not occur until >65 μm. The arithmetic average is shown at the bottom of the panel. In general, as the fiber diameter increases relative to the beam width, there is a greater probabililty of measuring diffraction angles, which do not represent average sarcomere spacing. Fig. 8 illustrates this phenomenon for a 50-μm diam fiber. The scan using the 1-mm beam does not deviate by more than 3% from theoretical. Conversely, the scan using the 100-μm beam shows two major shifts in position between the 11th and 13th scans and between the 18th and 20th scans.

DISCUSSION

The purpose of this investigation has been to characterize and test the conditions under which light diffraction provides the best measure of the average sarcomere length within an illuminated region. The major conclusions are the following.

(*a*) Experimental conditions under which diffraction patterns are obtained can influence the type of information obtained from such measurements. The intensity of Bragg reflections is determined by the thickness of the fiber (number of myofibrils) illuminated. The intensity of grating diffraction is determined by the width of the beam illuminating the fiber.

(*b*) The superposition of Bragg and grating diffraction determines the intensity and position of a diffracted order.

(*c*) The best conditions for measuring sarcomere length in single skeletal muscle fibers are to use small (<60 μm) fibers and large (1 mm) incident beams.

The grating equation at normal incidence

$$n\lambda = d \sin \theta_d \quad (5)$$

is commonly used to determine sarcomere length in muscle. The validity of average sarcomere length values obtained using this equation depends on the assumption that all sarcomeres in the illuminated region contribute equally to the diffracted intensity. In this case, the accuracy of sarcomere length determination will be limited by the local sarcomere length variation (Morgan, 1978). Major problems of interpretation arise when clusters of sarcomeres dominate the diffraction pattern to such an extent that the position of the diffraction order does not yield a representative value for the region. Such phenomena have been demonstrated by Rüdel and Zite-Ferenczy (1979*a,b*). Their results have cast doubt on the results obtained from experiments using light diffraction. In an earlier investigation (Baskin et al., 1981), we showed that the diffraction phenomenon in muscle can be represented as the superposition of grating diffraction by sarcomeres distributed along the fiber axis and three-dimensional diffraction by myofibrils arranged perpendicularly to the fiber axis.

Strong support for the above proposal has been obtained in the present investigation, where interaction between the two types of diffraction has been demonstrated. The theory of Yeh et al. (1980) suggested that the two parameters of interest in this investigation would be beam width and fiber thickness (see Theoretical Background). Thus, by varying these parameters and examining the resulting diffraction patterns, we have concluded that grating information (i.e., sarcomere length) can be made to dominate the diffraction pattern if the beam width-to-fiber ratio is relatively large (>10).

Note that although the theory of Yeh et al. (1980) is only strictly applicable to the case of a weak or thin phase grating because multiple scattering effects were not considered, we feel that the discussion presented here is valid for two reasons.

(*a*) Thick grating theory (e.g., the coupled-mode theory of Magnusson and Gaylord [1977]) predicts dumping of intensity from lower to higher diffraction orders. Diffraction patterns resulting from such thick gratings are characterized by a variation in intensity of the diffracted orders, which deviates significantly from the simple damped oscillatory type typically observed in skeletal muscle (see for example, Fig. 1 of Raman and Nath [1935]). It thus appears that multiple scattering in the single fiber system does not significantly affect the centroid of the peaks from the resultant diffraction pattern.

(*b*) Thick grating theory suggests that the intensity profiles in Fig. 2 be modified according to the effects of multiple scattering within the fiber. As mentioned above, multiple scattering serves to modulate the intensity of a diffracted order but not the centroid of the order. Intensity changes that result from multiple scattering would thus not affect the validity of this discussion because, in practice, diffraction angle and not intensity is measured to determine sarcomere length.

ω-Scans

The increased fine structure in angle scans obtained with larger fibers and smaller beams (Fig. 4) suggests that Bragg effects can best be expressed when the population of sarcomeres illuminated is relatively small. However, this type of experiment is difficult to interpret because, in comparing the results obtained with large and small beams, the magnitude and quality of the populations illuminated are different. Thus, it may not be correct to assign a correspondence between peaks obtained in ω-scans with large and small beams. Increased fine structure may occur as a result of the complex interference that occurs when neither Bragg nor grating diffraction dominate (Fig. 2 *D*) or as a result of the typical variation of sarcomere length within the illuminated region. Another reason for increased fine structure may be that because the sample size is smaller, less statistical smoothing occurs. Because each minor peak in the ω-scan does not necessarily represent an individual population of myofibrils but may represent the resultant intensity of many different populations (see Baskin et al., 1981), changing the sample size may affect the ω-scan in ways that are not obvious.

Intensity and Position Variation Across an Order as a Function of Incident Angle

Because a diffracted order follows the position predicted by the grating equation for arbitrary incident angle, there is additional direct evidence that under certain conditions a skeletal muscle fiber behaves as a weak phase grating to incident laser light. The degree to which this relationship holds true seems to be dependent on the ratio of beam width-to-fiber diameter. Under conditions where this ratio is small (~1, Figs. 5 *B*, 8, and 9), the diffracted order can show considerable splitting and fluctuation in position. This splitting and positional fluctuation is likely due to Bragg diffraction, which can be expressed because of the small number of sarcomeres illuminated. Sarcomere length measurements made under these conditions would not provide as reliable an average sarcomere length value as those taken under the converse situation (large beam diameter-to-fiber ratio, Figs. 4 *A*, 5 *A* and 7). With the small beam and large fibers there is an increased probability of obtaining nonrepresentative sarcomere length values. This is manifest in the difference between average deviation values for large (1.45%, 1.22%) and small (2.94%, 1.44%) beams. Note that in the case of the large beam, even measurements taken on the large fibers only show an average deviation of 1.45%. In addition, the diffracted order shows little if any splitting and closely follows the movement predicted for a one-dimensional grating. Sarcomere length measurements taken under these conditions

would thus be representative of the average sarcomere length within the region. As is shown in Fig. 10, based on our investigations, the approximate upper limit for fiber diameter, which would yield reliable average sarcomere length data, is ~65 μm.

An alternative explanation for the theoretical basis of the diffraction pattern was presented by Judy et al. (1982). This theoretical treatment associates the fine structure in the diffraction pattern with individual sarcomere populations. Experimental support for this theory was given by Tameyasu et al. (1982) who showed that the distance between the fine structure lines is distributed about a mean of 12–14 nm.

Given this approach, an alternate explanation of our data can be offered. As incident angle is varied and the illuminated volume changes, different sarcomere populations contribute to the diffraction pattern. Because this volume change is most pronounced for the small beam and large fiber, it may be argued that the increased fine structure and increased apparent sarcomere length deviation observed are due to changes in sampled population as a function of incident angle. This explanation requires that adjacent populations of sarcomeres exist with sarcomere lengths as different as 3–5% as these differences were measured with the small beam and large fibers.

Regardless of the theoretical basis for the diffraction phenomenon in muscle, we have shown here that the conditions under which sarcomere length measurements are made can influence the reliability of the data. An example is found in the report of Rüdel and Zite-Ferency (1979*b*), where they show that Bragg effects may cause an apparent 2% increase in sarcomere length in one diffracted order, while the other order indicates a decrease of ~4%. Our results support the hypothesis that Bragg effects of this magnitude can be observed. Their experiments were carried out under conditions where Bragg effects would be expected to dominate the diffraction pattern: large (120 μm) fiber and small (100 μm) beam.

In addition to using small diameter fibers and large beams, other methods of minimizing Bragg effects have been implemented. Goldman and Simmons (1979) have employed a system that illuminates the fiber at a variety of incident angles, thus precluding the possibility of satisfying the Bragg condition. In addition, Goldman (1983) has recently implemented a device that illuminates the fiber with polychromatic light, thereby avoiding constructive interference from skew planes within the fiber.

The authors would like to thank Drs. T. A. Cahill, L. E. Ford, and Y. E. Goldman for their helpful discussion during the preparation of this manuscript. In addition, we thank the referees of this Journal for their helpful comments. We are also indebted to Martha Corcoran for her skilled technical assistance.

This research was aided by the National Science Foundation grant PCM 79-03256 to R. J. Baskin and by the National Institutes of Health grant 5RO1AM26817 to Y. Yeh. R. L. Lieber was a National Insititutes of Health Predoctoral Fellow.

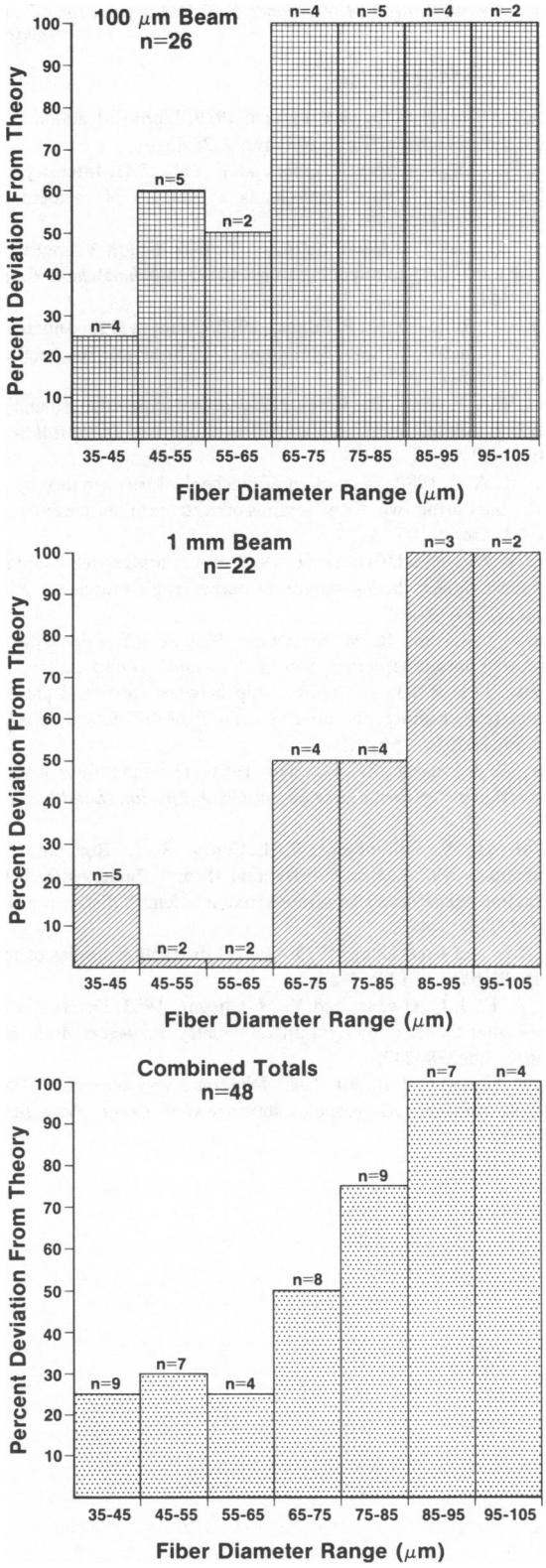

FIGURE 10 Summary of data. *Vertical axes*: percent of fibers in a given diameter range that deviate from ideal (Eq. 4) by more than 3%. *Horizontal axes*: fiber diameter range. Number of fibers in each range shown above bar. *Upper*: summary of data using 100-μm beam, $n = 26$. *Middle*: summary of data using 1-mm beam, $n = 22$. *Bottom*: arithmetic average of data, $n = 48$. Note that as the fiber diameter increases, the probability of obtaining errant information increases.

Received for publication 24 November 1982 and in final form 7 August 1983.

REFERENCES

Baskin, R. J., K. P. Roos, and Y. Yeh. 1979. Light diffraction study of single skeletal muscle fibers. *Biophys. J.* 28:45–64.

Baskin, R. J., R. L. Lieber, T. Oba, and Y. Yeh. 1981. Intensity of light diffraction from striated muscle as a function of incident angle. *Biophys. J.* 36:759–773.

Borejdo, J., and P. Mason. 1976. Sarcomere length changes during stimulation of frog semitendinosus muscle. *J. Mechanochem. Cell Mot. 3:155–161.*

Cleworth, D. R., and K. A. P. Edman. 1972. Changes in sarcomere length during isometric tension development in frog skeletal muscle. *J. Physiol. (Lond.).* 227:1–17.

Edman, K. A. P. 1966. The relation between sarcomere length and active tension in isolated semitendinosus fibres of the frog. *J. Physiol. (Lond.).* 183:407–417.

Edman, K. A. P. 1980. Depression of mechanical performance by active shortening during twitch and tetanus of vertebrate muscle fibres. *Acta Physiol. Scand.* 109:15–26.

Flitney, F. W., and D. G. Hirst. 1978. Cross-bridge detachment and sarcomere "give" during stretch of active frog's muscle. *J. Physiol. (Lond.).* 276:449–465.

Goldman, Y. E., and R. M. Simmons. 1979. A diffraction system for measuring muscle sarcomere length. *J. Physiol. (Lond.).* 287:5–6P.

Goldman, Y. E. 1983. The relationship between force and velocity of sarcomere shortening measured by white light diffraction. *Biophys. J.* 41(2, Pt. 2):257*a*. (Abstr.)

Huxley, A. F., and L. D. Peachey. 1961. The maximum length for contraction in vertebrate striated muscle. *J. Physiol. (Lond.).* 156:150–165.

Judy, M. M., V. Summerour, T. LeConey, R. L. Roa, and G. H. Templeton. 1982. Muscle diffraction theory. Relationship between diffraction subpeaks and discrete sarcomere length distributions. *Biophys. J.* 37:475–487.

Kawai, M., and I. D. Kunz. 1973. Optical diffraction studies of muscle fibers. *Biophys. J.* 13:857–876.

Leung, A. F., J. C. Hwang, and Y. M. Cheung. 1983. Determination of myofibrillar diameter by light diffractometry. *Pfluegers Arch. Eur. J. Physiol.* 396:238–242.

Lieber, R. L., and R. J. Baskin. 1980. Direct memory access of diffraction patterns from striated muscle. A software view. *Comp. Prog. Biomed.* 13:27–31.

Lieber, R. L., R. J. Baskin, and Y. Yeh. 1981. The use of laser diffraction to measure sarcomere length. *Biophys. J.* 33(2, Pt. 2):223*a* (Abstr.)

Magid, A., and M. K. Reedy. 1980. X-ray diffraction observations of chemically skinned frog skeletal muscle processed by an improved method. *Biophys. J.* 30:27–40.

Magnusson, R., and T. K. Gaylord. 1977. Analysis of multiwave diffraction of thick gratings. *J. Opt. Soc. Am.* 67:1165–1170.

Morgan, D. L. 1978. Predictions of some effects on light diffraction patterns of muscles produced by areas with different sarcomere lengths. *Biophys. J.* 21(2, Pt. 2):88*a* (Abstr.)

Moss, R. L., and W. Halpern. 1977. Elastic and viscous properties of resting frog muscle. *Biophys. J.* 17:213–228.

Oba, T., R. J. Baskin, and R. L. Lieber. 1981. Light diffraction studies of active muscle fibers as a function of sarcomere length. *J. Musc. Res. Cell Mot.* 2:215–224.

Paolini, P. J., R. Sabbadini, K. P. Roos, and R. J. Baskin. 1976. Sarcomere length dispersion in single skeletal muscle fibers and fiber bundles. *Biophys. J.* 16:919–929.

Raman, C. V., and N. S. N. Nath. 1935. The diffraction of light by high frequency sound waves: Part I. *Proc. Indian Acad. Sci. Sect. A* 2:406–412.

Roos, K. P., R. J. Baskin, R. L. Lieber, J. W. Cline, and P. J. Paolini. 1980. Digital data acquisition and analysis of striated muscle diffraction patterns with a direct memory access microprocessor system. *Rev. Sci. Inst.* 51:762–767.

Rüdel, R., and F. Zite-Ferenczy. 1979*a*. Interpretation of light diffraction by cross-striated muscle as Bragg reflexion of light by the lattice of contractile proteins. *J. Physiol. (Lond.).* 290:317–330.

Rüdel, R., and F. Zite-Ferenczy. 1979*b*. Do laser diffraction studies on striated muscle indicate stepwise sarcomere shortening? *Nature (Lond.). 278:573–575.*

Schoenberg, M., J. B. Wells, and R. J. Podolsky. 1974. Muscle compliance and the longitudinal transmission of mechanical impulses. *J. Gen. Phys.* 64:623–642.

Tameyasu, T., N. Ishide, and G. H. Pollack. 1982. Discrete sarcomere length distribution in skeletal muscle. *Biophys. J.* 37:489–492.

Walcott, B., and M. M. Dewey. 1980. Length-tension relation in limulus striated muscle. *J. Cell Biol.* 87:204–208.

Yeh, Y., R. J. Baskin, R. L. Lieber, and K. P. Roos. 1980. Theory of light diffraction by single skeletal muscle fibers. *Biophys. J.* 29:509–522.

Zite-Ferenczy, F., and R. Rüdel. 1978. A diffractometer using a lateral effect photodiode for the rapid determination of sarcomere length changes in cross-striated muscle. *Pfluegers Arch. Eur. J. Physiol.* 374:97–100.